Environmental Science & Technology

Policy Analysis

Natural gas fugitive emissions rates constrained by global atmospheric methane and ethane

Stefan Schwietzke, W. Michael Griffin, H. Scott Matthews, and Lori M. P. Bruhwiler

Environ. Sci. Technol., **Just Accepted Manuscript** • Publication Date (Web): 19 Jun 2014

Downloaded from http://pubs.acs.org on June 26, 2014

Just Accepted

"Just Accepted" manuscripts have been peer-reviewed and accepted for publication. They are posted online prior to technical editing, formatting for publication and author proofing. The American Chemical Society provides "Just Accepted" as a free service to the research community to expedite the dissemination of scientific material as soon as possible after acceptance. "Just Accepted" manuscripts appear in full in PDF format accompanied by an HTML abstract. "Just Accepted" manuscripts have been fully peer reviewed, but should not be considered the official version of record. They are accessible to all readers and citable by the Digital Object Identifier (DOI®). "Just Accepted" is an optional service offered to authors. Therefore, the "Just Accepted" Web site may not include all articles that will be published in the journal. After a manuscript is technically edited and formatted, it will be removed from the "Just Accepted" Web site and published as an ASAP article. Note that technical editing may introduce minor changes to the manuscript text and/or graphics which could affect content, and all legal disclaimers and ethical guidelines that apply to the journal pertain. ACS cannot be held responsible for errors or consequences arising from the use of information contained in these "Just Accepted" manuscripts.

ACS Publications
High quality. High impact.

Environmental Science & Technology is published by the American Chemical Society.
1155 Sixteenth Street N.W., Washington, DC 20036
Published by American Chemical Society. Copyright © American Chemical Society.
However, no copyright claim is made to original U.S. Government works, or works produced by employees of any Commonwealth realm Crown government in the course of their duties.

Natural gas fugitive emissions rates constrained by global atmospheric methane and ethane

Stefan Schwietzke*[,†,ϟ], W. Michael Griffin[†,‡], H. Scott Matthews[†,§], Lori M. P. Bruhwiler[#]

[†] Department of Engineering and Public Policy, Carnegie Mellon University, Baker Hall 129, 5000 Forbes Avenue, Pittsburgh, PA 15213, United States

[‡] Tepper School of Business, Carnegie Mellon University, 5000 Forbes Avenue, Pittsburgh, PA 15213, United States

[§] Department of Civil and Environmental Engineering, Carnegie Mellon University, Porter Hall 123A, 5000 Forbes Avenue, Pittsburgh, PA 15213, United States

[#] NOAA Earth Systems Research Laboratory, 325 Broadway GMD1, Boulder, CO 80305, United States

Corresponding Author

* Phone: (303) 497-5073. Fax: (303) 497-5590. E-mail: stefan.schwietzke@noaa.gov.

Abstract

The amount of methane emissions released by the natural gas (NG) industry is a critical and uncertain value for various industry and policy decisions, such as for determining the climate implications of using NG over coal. Previous studies have estimated fugitive emissions rates (FER)

– the fraction of produced NG (mainly methane and ethane) escaped to the atmosphere – between 1-9%. Most of these studies rely on few and outdated measurements, and some may represent only temporal/regional NG industry snapshots. This study estimates NG industry representative FER using global atmospheric methane and ethane measurements over three decades, and literature ranges of (i) tracer gas atmospheric lifetimes, (ii) non-NG source estimates, and (iii) fossil fuel fugitive gas hydrocarbon compositions. The modeling suggests an upper bound global average FER of 5% during 2006–2011, and a most likely FER of 2-4% since 2000, trending downward. These results do not account for highly uncertain natural hydrocarbon seepage, which could lower the FER. Further emissions reductions by the NG industry may be needed to ensure climate benefits over coal during the next few decades.

Introduction

The effectiveness of mitigating climate change using natural gas (NG) as a bridge to a renewable energy-dominated economy has been challenged by some[1,2], suggesting that methane (CH_4) emissions from NG systems could outweigh reduced CO_2 emissions compared to coal use. Other studies[3–6] indicate that U.S. emissions inventories underestimate CH_4 emissions from the oil and gas industry. The increased tapping of shale formations and other unconventional NG sources – increasing production in North America and exploration activities worldwide using new technologies – adds urgency to the problem.

The U.S. Environmental Protection Agency recently amended air regulations for the oil and gas industry including targets for capturing NG that currently escapes to the atmosphere[7]. Accurately determining CH_4 emissions that are representative of the NG industry is key for this and future policies, but it is also challenging due to the size and complexity of the NG industry[8,9]. CH_4 is

40 released to the atmosphere, intentionally (e.g., venting) and unintentionally (leaks), throughout the
41 NG life cycle, which includes extraction, processing, transport, and distribution. The magnitude
42 of life cycle CH_4 emissions is sometimes reported as the NG fugitive emissions rate (FER), defined
43 here as the percentage of dry production – mainly CH_4 – that is lost throughout its life cycle.
44 Most literature FER estimates were generated using bottom-up approaches, i.e., aggregating
45 measurements and engineering estimates at different life cycle stages. Previous bottom-up studies
46 by these[10,11] and other authors[1,8,9] showed that outdated and small sample size measurement data
47 largely contribute to FER uncertainty. Local air sampling studies near NG production facilities
48 complement the bottom-up studies[3,4], but they only represent a regional and temporal snapshot of
49 the larger industry. High FER of 6-9% were reported recently using both approaches[1,4].
50 This work estimates global average FER with a top-down approach that uses long-term (1984-
51 2011) global atmospheric CH_4 and ethane (C_2H_6) measurements to evaluate the representativeness
52 of previous bottom-up results. These tracer gas species are the main hydrocarbon components of
53 NG[12]. Unlike CH_4, C_2H_6 is not thought to have microbial sources[13,14], so its atmospheric abundance
54 can be a useful constraint on FER. A third tracer – the carbon isotope $\delta^{13}C\text{-}CH_4$ – was employed,
55 which provides a stronger constraint for FER than CH_4 alone. $\delta^{13}C\text{-}CH_4$ observations[15] were used
56 to exploit the fact that the isotopic values of observed atmospheric CH_4 are the result of the
57 magnitudes and the distinct isotopic signatures of the various CH_4 sources. For instance, CH_4
58 emissions from fossil fuel (FF) sources are significantly less depleted in $\delta^{13}C\text{-}CH_4$ compared to
59 microbial sources, such as wetlands[16]. Previous top-down studies have estimated global or national
60 FF CH_4 and C_2H_6 emissions[5,13,17] using complex 3D models of the atmosphere based on (i) *a priori*
61 knowledge of the approximate locations of different emissions, and (ii) spatially distributed
62 atmospheric measurements. However, using observations to distinguish emissions from NG, oil,

and coal is difficult due to close relative proximity of these sources[6]. Quantifying the NG source is necessary to estimate FER. A detailed global bottom-up oil and coal CH_4 and C_2H_6 emissions inventory[18] was developed for this study to isolate NG emissions from those associated with oil and coal.

Methods

Global NG CH_4 and C_2H_6 emissions and uncertainties were estimated annually over the period 1985-2011 using a top-down mass balance as the difference between total emissions and other anthropogenic and natural sources. The mass balance model treats the global atmosphere as a single box, which conserves the global mass of the emissions sources and sinks (and resulting atmospheric mixing ratios), eliminating the need for complex global transport of emissions. Total annual emissions ranges were based on (i) CH_4 and C_2H_6 atmospheric measurement data from NOAA's[19] and UC-Irvine's[13] global observation networks (see SI section 1 for global average annual mixing ratios), respectively, (ii) literature atmospheric $\delta^{13}C$-CH_4 data[15], and (iii) literature ranges of global average atmospheric CH_4 and C_2H_6 lifetimes (both largely dependent on reaction with OH)[20–24] summarized in the following subsection. The magnitudes of the uncertain anthropogenic and natural CH_4 and C_2H_6 sources were derived using a wide range of literature estimates (SI section 2) and the above-mentioned oil and coal inventory[18]. Given the resulting annual NG CH_4 and C_2H_6 top-down estimates, FER was estimated using global NG production statistics in combination with thousands of NG composition samples specifying NG CH_4 and C_2H_6 contents worldwide.

Inter-annual variability in the OH abundance and the non-FF source strength affects FER estimates in a given year. For instance, declining OH or non-FF emissions would increase FER. This study is primarily interested in the long-term FER trajectory. We therefore only accounted

for inter-annual variations in the above model parameters where the literature indicates a long-term trend (such as in CH_4 and C_2H_6 mixing ratios shown in SI section 1). Given the lack of evidence for long-term trends in the global OH abundance[25] and non-FF emissions[13,17] (for details see SI sections 1 and 2, respectively), inter-annual variation in non-FF emissions sources was neglected.

Using a relatively simple model, a range of scenarios was explored in order to evaluate what may be learned from the atmospheric observations, including the maximum possible global average FER. Finally, mass balance FER estimates were substantiated using the existing 3D global chemistry transport model TM5[26] implemented in the CarbonTracker-CH_4 (CT-CH_4) assimilation system[27]. This was achieved by simulating transport of emissions throughout the global atmosphere for selected FER scenarios. The resulting CH_4 mixing ratios were then compared with observations from the global networks[13,19], thereby adding spatial information not available using the mass balance model.

Global mass balance (box-model)

The global annual mass balance for CH_4 and C_2H_6 in year *t* was formulated as:

$$z_{CH4,t} = z_{CH4,t,AgW} + z_{CH4,t,Nat} + z_{CH4,t,BBM} + z_{CH4,t,Oil} + z_{CH4,t,NG} + z_{CH4,t,Coal/Ind} \quad \textbf{Eq. 1,}$$

$$z_{C2H6,t} = z_{C2H6,t,BBE} + z_{C2H6,t,BFC} + z_{C2H6,t,Oil} + z_{C2H6,t,NG} + z_{C2H6,t,Coal} \quad \textbf{Eq. 2,}$$

where $z_{CH4,t}$ and $z_{C2H6,t}$ are the total annual global CH_4 and C_2H_6 emissions, respectively. The CH_4 emissions sources include agriculture/waste/landfills (*AgW*), natural sources (*Nat*), biomass burning methane (*BBM*), oil life cycle fugitive emissions (*Oil*; CH_4 and C_2H_6), NG life cycle fugitive emissions (*NG*; CH_4 and C_2H_6), and coal life cycle fugitive and "other energy and industry" emissions (*Coal/Ind*). The C_2H_6 emissions sources also include biomass burning ethane

(*BBE*; savanna and grassland fires, tropical and extratropical forest fires, agricultural residue burning), biomass fuel combustion (*BFC*), and coal life cycle C_2H_6 emissions (*Coal*; see below for "other energy and industry" C_2H_6 emissions). The literature-based CH_4 and C_2H_6 emissions ranges are summarized in the Methods subsections (non-FFs and FFs) below. The system boundaries for the CH_4 sources vary slightly among studies, but are largely consistent with those described for modeling with TM5 (SI Table S1). Mass balances were solved for $z_{CH4,t,NG}$ and $z_{C2H6,t,NG}$ independently using the ranges for all other source categories. The annual emissions $z_{CH4,t}$ were estimated using Eq. 4, which is the solution to differential Eq. 3, giving $z_{CH4,t}$. The annual emissions $z_{C2H6,t}$ were estimated using Eq. 5:

$$dC_{CH4}/dt = z_{CH4,t} - 1/\tau * C_{CH4,t} \quad \textbf{Eq. 3,}$$

$$z_{CH4,t} = \left(C_{CH4,t} - C_{CH4,t-1} * e^{-\frac{1}{\tau}}\right) * \left(\tau * \left(1 - e^{-\frac{1}{\tau}}\right)\right)^{-1} \quad \textbf{Eq. 4,}$$

$$z_{C2H6,t} = C_{C2H6,t} * SF_{C2H6} \quad \textbf{Eq. 5,}$$

where $C_{CH4,t}$ is the annually observed global average CH_4 dry air mole fraction (in ppb) in year t multiplied by the conversion factor 2.767 Tg CH_4/ppb[28] in order to convert mole fractions to mass units for the global atmosphere (see SI section 1 for details). For the global average atmospheric lifetime of CH_4, τ, a range of 9.1-9.7 years was chosen, which includes the mean values from four recent studies[20–23]. The scaling factor SF_{C2H6} converts the annually observed global average C_2H_6 dry air mole fraction $C_{C2H6,t}$ into the annual emissions burden $z_{C2H6,t}$, which is based on 3D-modeling[24] and has been applied recently elsewhere[13]. Given uncertainties of up to 45% due to the reaction rate with and mixing ratios of OH[24], the average and upper bound values of SF_{C2H6} (corresponding to a higher global budget for estimating upper bound FER), 0.018 and 0.026 Tg C_2H_6/ppt, respectively, were used.

The global mass balance using atmospheric $\delta^{13}C$-CH_4 measurements constrains FER based on the fact that the various CH_4 sources carry distinct isotopic CH_4 signatures. The ^{13}C:^{12}C ratio of CH_4, δ (in ‰), can be expressed as[29]:

$$\delta = \left(R_{Sample}/R_{Standard} - 1\right) * 1000 \quad \textbf{Eq. 6,}$$

where $R = (Rare\ isotope\ /\ Abundant\ isotope)$. The global mass balance for three CH_4 source categories can be formulated for each year as[16]:

$$z_{CH4,t} = z_{Mic,t} + z_{FF,t} + z_{BBM,t} \quad \textbf{Eq. 7,}$$

$$\delta_q z_{CH4,t} = \delta_{Mic} * z_{Mic,t} + \delta_{FF} * z_{FF,t} + \delta_{BBM} * z_{BBM,t} \quad \textbf{Eq. 8,}$$

where $z_{Mic,t}$, $z_{FF,t}$, and $z_{BBM,t}$ refer to the microbial, FF, and BBM fraction of total annual CH_4 emissions, respectively, and $z_{Mic,t}$ includes all natural and agriculture/waste/landfills sources. The different CH_4 emissions sources are aggregated to only three emissions categories in order to avoid an under-constrained system of two linear equations (Eq. 7 and Eq. 8). The equation system is solved for $z_{Mic,t}$ and $z_{FF,t}$ as an optimization problem (Eq. 10 through Eq. 15), and $z_{BBM,t}$ is considered at least 25 Tg CH_4/yr (see literature review in SI section 2). The literature provides wide ranges of source- (and geography-) specific isotopic signatures. For instance, Finnish subarctic wetlands range between –65 ‰ and –69 ‰[30] compared to –51 ‰ and –53 ‰ from landfills[16]. West Siberian NG associated with oil production (high CH_4 content) has been measured around -50 ‰[30], whereas mature dry gas can range approximately -20 ‰[31]. The isotopic signatures δ_{Mic}, δ_{FF}, and δ_{BBM} in this model are based on weighted averages of each emissions category from 13 literature sources[16], and lie within the range of –59 to –63 ‰, –38 to –42 ‰, and –22 to –26

‰, respectively. The total annual CH_4 emissions burden $z_{CH4,t}$ is the same as in Eq. 4, and the flux weighted mean isotopic ratio of all CH_4 sources[29] is:

$$\delta_{q,t} = \alpha\delta_a + \varepsilon - \frac{\varepsilon(1+\delta_a/1000)}{z_{CH4,t}} * \frac{dC_{CH4,t}}{dt} + \frac{d\delta_a}{dt} * \frac{C_{CH4,t}}{z_{CH4,t}} \quad \textbf{Eq. 9},$$

where $\alpha = (1 + \varepsilon / 1000)$ is the isotopic fractionation factor associated with photochemical CH_4 destruction, for which ε = -6.3 ‰[16]. As described in more detail in SI section 1, the global annual means of measured δ_a range between -47.0 ‰ and -47.3 ‰ throughout 1988–2011[15,32,33]. Given (i) the lack of pre–1988 data, (ii) the reliance on unpublished post-2006 data[32], (iii) and the low sensitivity of the above δ_a range on FER (see SI section 3.1), this model assumes a constant δ_a of -47.1 ‰. Eq. 7 and Eq. 8 were re-arranged to give:

$$z_{FF,t} = \frac{\delta_{q,t} * z_{CH4,t} - \delta_{Mic} * \left(z_{CH4,t} - z_{BBM,t}\right) - \delta_{BBM} * z_{BBM,t}}{\delta_{FF} - \delta_{Mic}} \quad \textbf{Eq. 10,}$$

$$z_{Mic,t} = z_{CH4,t} - z_{FF,t} - z_{BBM,t} \quad \textbf{Eq. 11},$$

where units for $z_{CH4,t}$ and δ are Tg CH_4/yr and ‰, respectively. The optimization problem is to minimize Eq. 10, such that:

$$z_{BBM,t} \geq 25 \quad \textbf{Eq. 12,}$$

$$-59 \geq \delta_{Mic} \geq -63 \quad \textbf{Eq. 13},$$

$$-38 \geq \delta_{FF} \geq -42 \quad \textbf{Eq. 14},$$

$$-22 \geq \delta_{BBM} \geq -26 \quad \textbf{Eq. 15}.$$

Eq. 12 ensures that there are only two unknowns in the problem of two linear equations. CH_4 emissions from NG $z_{C13CH4,t,NG}$ (based on isotope observations) are the difference between FF emissions from the isotope mass balance and coal/oil emissions, which are described in more detail below:

$$z_{C13CH4,t,NG} = z_{FF,t} - z_{CH4,t,Coal/Ind} - z_{CH4,t,Oil} \quad \textbf{Eq. 16}.$$

Finally, FER is estimated using Eq. 17 through Eq. 19:

$$FER_{CH4,t} = z_{CH4,t,NG}/\left(P_{dry,t} * WF_{down,CH4,t}\right) \quad \textbf{Eq. 17,}$$

$$FER_{C2H6,t} = z_{C2H6,t,NG}/\left(P_{dry,t} * WF_{down,C2H6,t}\right) \quad \textbf{Eq. 18},$$

$$FER_{C13CH4,t} = z_{C13CH4,t,NG}/\left(P_{dry,t} * WF_{down,CH4,t}\right) \quad \textbf{Eq. 19},$$

where $P_{dry,t}$ is the global dry production of NG[34] converted from volume to weight units (see our bottom-up inventory[18] for details), and $WF_{down,CH4,t}$ and $WF_{down,C2H6,t}$ are the downstream NG weight fractions of CH_4 and C_2H_6, respectively.

Global 3D model

Three-dimensional forward simulations of CH_4 emissions using the global chemistry transport model TM5[26] complement the box-model approach. Forward simulations in this work cover the period 1989-2011, and measurements are the same as used for the box-model. The following five different zones were distinguished in order to analyze the spatial differences ignored in the box-model: polar Northern Hemisphere (PNH, 53.1°N-90°N), temperate Northern Hemisphere (TNH, 17.5°N-53.1°N), the tropics (17.5°S-17.5°N), temperate Southern Hemisphere (TSH, 17.5°S-53.1°S), and polar Southern Hemisphere (PSH, 53.1°S-90°S). These zones are pre-defined in CT-

186 CH_4[27], and briefly discussed in SI section 3.2. Emissions were simulated for 11 individual CH_4
187 source/sink categories including NG, oil, coal/industry, wetlands, soils, oceans, termites, wild
188 animals, agriculture/waste/landfills, and biomass burning methane (all as described above).
189 Emissions were simulated for each source separately, which allows tracking the individual
190 contributions of total CH_4 mixing ratios. Estimating source-specific contributions is key for
191 analyzing the underlying causes of potential spatial differences between simulations and
192 observations. These spatial differences mainly occur because the various sources emit in specific
193 world regions, which helps to distinguish emissions sources using the measurements from the
194 global monitoring networks.

195 **Model values of non-fossil fuel emissions categories based on literature review**

196 This section describes the range of non-NG CH_4 and C_2H_6 emissions values chosen as inputs in
197 the box-model (Eq. 1, Eq. 2, Eq. 10, and Eq. 11) and the 3D-model. Non-FF CH_4 emissions ranges
198 were selected based on five of the most recent inversion studies[27,35–38] and two literature
199 reviews[39,40], which is described in more detail in the SI (section 2), and summarized in Table 1. In
200 the box-model, most likely FER assumes total non-FF CH_4 sources of 400 Tg/yr (medium non-FF
201 scenario), and upper bound FER is associated with non-FF CH_4 sources of 265 Tg/yr (low non-FF
202 scenario). The corresponding medium and low scenario C_2H_6 estimates are 5.9 Tg/yr and 2.2
203 Tg/yr, respectively. High CH_4 and C_2H_6 scenarios were selected such that low and high values
204 represent a normal distribution around the medium values. Three-dimensional forward simulations
205 were carried out with TM5 for 8 individual non-FF CH_4 source/sink categories (totaling on average
206 385 Tg/yr). The global soil CH_4 sinks used in both models cover the range of literature values: 25
207 Tg/yr[36], 30 Tg/yr[35], and 38 Tg/yr[38]. The total non-FF emissions in the 3D simulation and in the
208 medium box-model scenario are very similar (difference is ~3% of global CH_4 budget), which

allows direct comparison of box-model results with the 3D-model (the same oil and coal estimates were used in both models).

Table 1: Summary of global non-FF emissions estimates used in 3D-forward-modeling (TM5) and ranges for box-modeling. Units are Tg/yr.

	CH_4					C_2H_6		
	Natural	**Ag/waste/ landfills**	**BBM**	**Soil sink** [i]	**Total**	**BBE**	**BFC**	**Total**
Box-model (const. over time [ii])								
low	130	130	25	-25	260	1.6	0.6	2.2
medium	182	200	43	-25	400	3.6	2.3	5.9
high	235	270	60	-25	540	5.2	4.0	9.2
3D-model (avg. 1980-2011)	215 [iii]	194 [iv]	16 [v]	-40	385	n/a	n/a	n/a

Notes: Ag – Agriculture; BBM - Biomass burning methane; BBE - Biomass burning ethane; BFC - Biomass fuel combustion; [i] Box-model data from[17], 3D-model data from[41]; [ii] Inter-annual variations during 1980-2011 were ignored due to lack of long-term trends in OH and non-FF sources, and focus on long-term FER trajectory (see also text above); [iii] Annual emissions and seasonal cycle from[42]; [iv] Annual emissions from[43], seasonal cycle from[44]; [v] Annual emissions from[45,46], seasonal cycle from[47].

Model values of fossil fuel emissions categories from bottom-up inventory

This section briefly summarizes the methods and data used to estimate CH_4 and C_2H_6 emissions from oil and coal production, processing and transport (in Eq. 1 and Eq. 2) as well as downstream NG composition (Eq. 17 through Eq. 19) applied in the box-model and the 3D-model. This summary is based on a global bottom-up FF inventory developed by these authors[18]. Here, only the general methodology and major parameters are reviewed. The inventory is based on country-level NG, oil, and coal production data[34], a range of literature emissions factors (EFs, see below for literature sources), and observational gas flaring data[48,49]. EFs describe the amount of

229 hydrocarbon gas emitted to the atmosphere per unit of fuel produced, and EFs are the basis for
230 comparing greenhouse gas (GHG) emissions among different fuels or technologies in life cycle
231 assessment. The inventory also includes hydrocarbon composition data from thousands of samples
232 including NG and oil wells, both of which produce NG and oil[12]. The hydrocarbon composition
233 data is necessary for deriving FER from estimated total amounts of global NG CH_4 ($z_{CH4,t,NG}$) and
234 C_2H_6 ($z_{C2H6,t,NG}$) emissions.

235 Emissions factors (EF) related to the oil life cycle were reviewed from four studies[50–53], which
236 span an order of magnitude. The EFs include fugitive emissions from oil production, processing,
237 and shipping as well as hydrocarbon emissions from incompletely flared gas. The EF selected from
238 these studies[51] is 50% below the mean of the lowest[52,53] and highest[50] literature EF. This selection
239 assures that the upper bound FER from the box-model is a conservative estimate, i.e., box-model
240 FER could be lower if oil emissions were in fact higher. Emissions from marketed (i.e., not
241 flared/vented or repressured) associated NG production at oil wells are counted towards FER. The
242 detailed procedure for allocating emissions between oil and NG production is described in the
243 bottom-up inventory[18]. Country-specific EFs related to the coal life cycle[50,54–56] distinguish
244 different types of coal production. Comparison of different global coal production estimates (and
245 Chinese coal production in particular) suggests that the total emissions estimate in the inventory
246 may be an underestimate. Thus, analogously to the oil emissions estimates above, FER could be
247 lower than box-model results if coal emissions were in fact higher.

248 Table 2 summarizes the results from the bottom-up inventory[18] including oil and coal CH_4 and
249 C_2H_6 emissions over different time periods as well as global average downstream NG hydrocarbon
250 composition (related to dry production statistics). Medium oil CH_4 emissions increase from 14
251 Tg/yr (mean during 1985-1999) to 17 Tg/yr (mean during 2006-2011), and medium coal/industry

252 CH_4 emissions increase from 48 Tg/yr to 61 Tg/yr over the same periods. Medium oil C_2H_6
253 emissions increase from 5.5 Tg/yr to 6.6 Tg/yr over the same periods, and coal/industry C_2H_6
254 emissions are relatively small given the low coal-bed gas C_2H_6 content[18]. Downstream NG CH_4
255 and C_2H_6 contents averaged throughout 1984-2011 range from 85-87 wt-% and 7.2-7.7 wt-%,
256 respectively, while C_2H_6 content decreased from 7.8–6.8 wt-% over this period due to increased
257 C_2H_6 extraction for NG liquids[18].
258
259 **Table 2:** Summary of oil and coal/industry CH_4 and C_2H_6 emissions, and downstream NG
260 composition in the bottom-up inventory[18].

		Units	CH_4			C_2H_6 [i]		
			1985-1999	2000-2005	2006-2011	1985-1999	2000-2005	2006-2011
Emissions								
Oil	low	Tg/yr	5	6	6	4.4	5.0	5.2
	medium		14	16	17	5.5	6.3	6.6
	high		41	48	51	7.6	8.8	9.2
Coal/Industry	low		43	44	55	0.0	0.0	0.0
	medium		48	49	61	0.3	0.3	0.4
	high		56	57	71	0.6	0.6	0.8
Composition								
Downstream NG [ii]	low	wt-%		85			7.2	
	medium			86			7.4	
	high			87			7.7	

261 Notes: [i] Ranges of oil and coal/industry C_2H_6 emissions are due to uncertainties in C_2H_6 content
262 of fugitive hydrocarbon emissions. [ii] Downstream NG composition was estimated for use with dry
263 production statistics (shows averages over 1985-2011) to estimate life cycle FER (as described
264 above). Results are based on a mass balance of upstream NG, downstream NG, and natural gas
265 liquids at the processing stage (see box-model Methods). Low and high values represent 95%-C.I.
266
267 Industry (public power and heat, other energy industries, transportation, residential and other
268 sectors, industrial processes, FF fires) emissions were adopted from EDGAR v4.2[43]. C_2H_6
269 emissions estimates from this source were unavailable, and were not accounted for in the box-
270 model. FER could in fact be lower than box-model results if industry is a significant C_2H_6 source.

Three different FER scenarios (ranging from 2-6% FER; see SI for details) were simulated in TM5 to analyze which FER is most consistent with spatially distributed observations.

Spatial distribution of CH_4 emissions

Spatial CH_4 emissions grid maps were developed in order to perform 3D simulations of the global atmosphere in TM5. A detailed description of the grid map development as well as the results is provided in the bottom-up inventory[18], and briefly summarized here. The spatial distribution of FF emissions *within* each country was adopted from EDGAR v4.2[43], which is based on population density and other proxies. The absolute FF emissions in the grid maps were scaled based on the FF estimates summarized in the previous subsection. Due to the emissions differences between this work and EDGAR for a given country, the spatial distribution of the scaled grid maps differs from EDGAR on a global scale, but not within individual countries. In contrast to FF, other source categories have a distinct seasonal emissions cycle. EDGAR's agriculture/waste/landfills category annual emissions grid maps were decomposed into monthly grid maps, and scaled to a seasonal cycle as defined in SI Table S1. Agriculture/waste/landfills annual totals were linearly extrapolated from 2008 (last year in EDGAR) to 2011 using the last 10 years available in EDGAR. Literature spatial CH_4 emissions distribution was adapted for natural[57,58] and BBM[47] categories.

Results

Global average FER from the NG life cycle was estimated in a top-down approach to better understand industry representative CH_4 emissions. This study is based on global spatially distributed CH_4, $\delta^{13}C$-CH_4, and C_2H_6 measurements over three decades. A global box-model was developed and an existing 3D emissions transport model was used to attribute total emissions to

different sources, thereby taking into account uncertainties in atmospheric lifetimes of measured species as well as non-NG source estimates.

Global box-model

The most likely global FER of 2-4% on average during 2004-2011 (Figure 1) is consistent for CH_4, $\delta^{13}C$-CH_4, and C_2H_6 observations. These estimates assume (i) mean literature emissions values for each of the other source categories listed above, and (ii) global total oil and coal CH_4 emissions from this study's emissions inventory (medium values in Table 2), which agree well (2.5% difference) with EDGAR[43], i.e., the commonly used *a priori* FF database in global top-down CH_4 modeling. The upper bound global FER averaged over the last five years of observations is 5.0% (4.4% in 2011) based on C_2H_6 observations (Figure 1). The upper bound assumes (i) a C_2H_6 lifetime corresponding to the largest global average sink in the literature, (ii) a lower bound FF C_2H_6 content (Table 2), and (iii) a lower bound BBE/BFC C_2H_6 source estimate (Table 1). Details of the budgetary implications of the upper bound FER relative to the literature are illustrated in SI Figure S8. Results indicate upper bound FER of ~6% in the early 2000s, mainly due to lower FF production compared to later years. Note that FER peaks shown for some years in Figure 1 are likely due to inter-annual variation in natural sources[13]. Our upper bound throughout 1985-1999 is on average 9.3% (SI Figure S7). This temporal decline in FER is consistent with earlier work suggesting a decrease in FF C_2H_6 emissions[13,14]. Emissions reductions per unit of production (FER) in this work imply industry efficiency improvements, although the decline would be less steep if coal and oil EFs also declined over time (increased oil and coal production over time are accounted for). Global average CH_4 and $\delta^{13}C$-CH_4 data provide weaker constraints for upper bound FER, mainly due to literature source estimate uncertainties. Assuming lower bound estimates for natural, agriculture/waste/landfills, and BBM sources *simultaneously* would

315 lead to FER of 8% or higher averaged during 2004-2011 (SI Figure S5). Yet, Figure 1 shows that
316 such high FER is inconsistent with the C_2H_6 data.
317

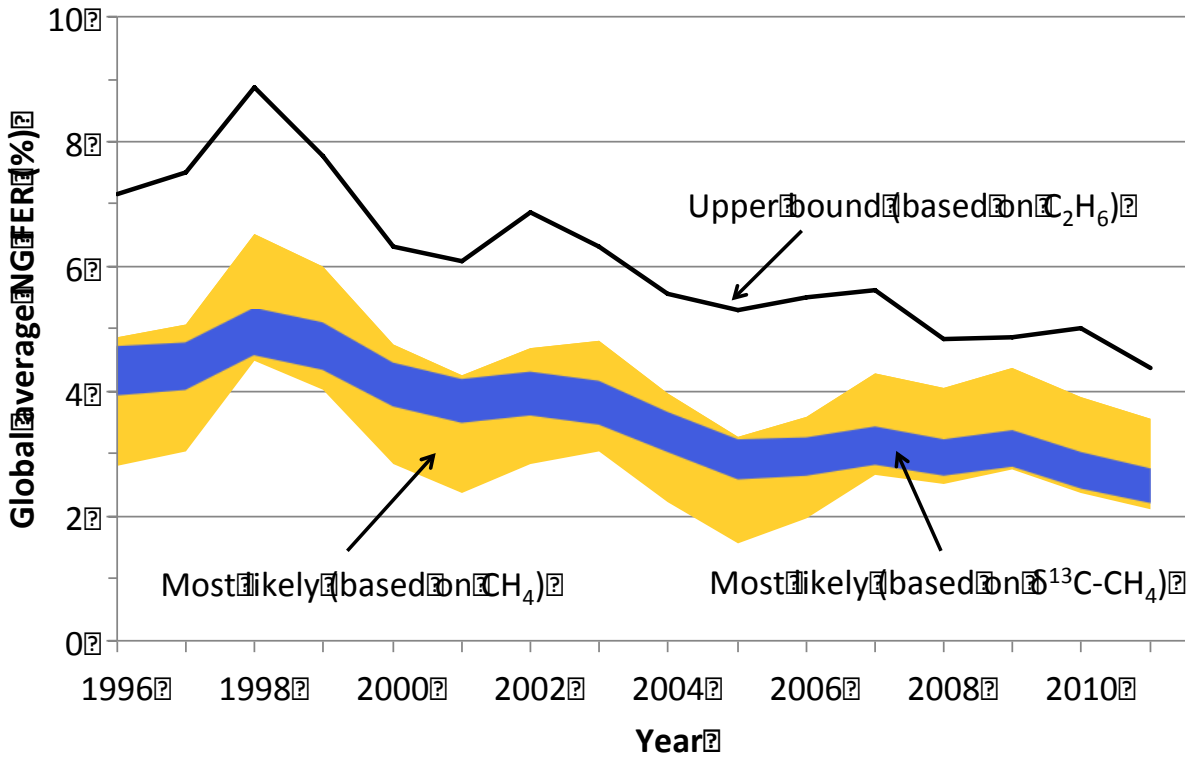

318

319 **Figure 1:** Summary of possible global NG fugitive emissions rates (FER) – in % of dry production
320 – based on a global mass balance using different tracer gases. The upper bound represents a
321 combination of assumptions from the literature including high global emissions (totaling 16.2 Tg
322 C_2H_6/yr on average since 2000 using UC-Irvine observations[13] and Rudolph[24] C_2H_6 lifetime
323 uncertainty) and low magnitude of other C_2H_6 sources (7.4 Tg C_2H_6/yr on average since 2000).
324 The orange and blue bands mark the range for CH_4 lifetimes between 9.1-9.7 years and mean
325 literature values of other CH_4 sources (totaling 467 Tg CH_4/yr on average since 2000 including
326 soil sink) using NOAA observations[19]. FER is shown for the longest consecutive observation time
327 series available (pre-1996 data are shown in SI Figures S5, S7).

328 Natural hydrocarbon seepage may be an additional significant source of atmospheric CH_4 and
329 C_2H_6 not currently accounted for in most top-down studies[17]. Visible macro-seeps, marine seepage,
330 micro-seepage, and geothermal/volcanic areas may contribute between 40-60 Tg CH_4/yr and 2-
331 4 Tg C_2H_6/yr globally[59]. While not included in Figure 1, adding 40 Tg CH_4/yr and 2 Tg C_2H_6/yr
332 in the model would reduce FER by about two percentage points (constant over time). The
333 magnitude of the above seepage estimates have been challenged[13]. Yet, having excluded any
334 seepage in our main results (Figure 1) emphasizes that our FER may be overestimated.
335 The decline in global FER is 0.1 and 0.3 percentage points per year since 1985 based on most
336 likely (CH_4 and $\delta^{13}C$-CH_4 observations) and upper bound results (C_2H_6 observations),
337 respectively. This assumes that the declines in measured C_2H_6 levels (or CH_4 growth rates[60]) are
338 attributed to NG emissions reductions. Kirschke *et al.*[17] find little if any long-term natural,
339 agriculture/waste/landfill, and BBM emissions reductions over this period. Kirschke *et al.*[17]
340 results, along with the findings presented here, suggest that the declines in measured mixing ratios
341 (or growth rates thereof) can be attributed to NG emissions reductions. This is also consistent with
342 recent top-down C_2H_6 studies[13,14] suggesting reductions in total FF emissions where Aydin *et al.*[14]
343 concluded that global declines in the C_2H_6 mixing ratios were due to decreased flaring and venting
344 of NG (see also SI Figure S8). Also, recent direct CH_4 measurements at 190 NG production sites
345 in the U.S. by Allen *et al.*[8] indicate lower overall CH_4 emissions from production (well pad)
346 activities than previous measurement data used in EPA's 2013 GHG inventory[51]. Note that
347 increased NG, oil, and coal production over time[61] was incorporated in the modeling presented
348 here. The FER decline may be less pronounced if oil and coal emissions per unit of production
349 also decreased since 1985. Atmospheric chemistry may also explain changes in CH_4 and C_2H_6
350 mixing ratios. However, Montzka *et al.*[62] recently found a small inter-annual atmospheric OH

variability of 2.3 ± 1.5% during 1998–2007, which suggests that increased sink strength is an unlikely alternative explanation for declining FER.

Global 3D-model

Most-likely FER estimates from the mass balance are supported by the global chemistry transport model TM5[26] and the spatial distribution of CH_4 mixing ratios as an indicator of source strength[63]. Using three different FER scenarios ranging from about 2-6% FER (see SI Table S4 and Figure S9), the TM5 was used to simulate spatially distributed CH_4 sources and sinks from 1989-2011. As shown in Figure 2a, the medium FER scenario is a reasonable fit globally throughout the 1990s (3-4% FER) compared to 3% and 5% in the box-model (SI Figure S5) for CH_4 lifetimes (τ) of 9.7 and 9.1, respectively. In the 2000s, TM5 suggests a most likely FER of ~3% dropping to just over 2% in 2010 compared to 2-4% in the box-model depending on τ. Given that τ used in TM5 is approximately 9.45, most likely estimates of both models agree within one percentage point FER.

The following spatial analysis is useful for investigating whether the *a priori* emissions source attribution (Tables 1 and 2) is reasonable, or if – for instance – underestimated FER scenarios were compensated by overestimated other source categories. Simulations and measurements across 41 latitudinal bands (intervals of 0.05 sine of latitude) are shown in Figure 2b as an indicator of the inter-hemispheric gradient (for year 2000; see SI Figure S10 for additional years). The spatial fit of simulations and measurements can be used as a proxy for the attribution of sources. About 96% of NG CH_4 emissions in the emissions grid maps simulated with TM5 are released in the Northern Hemisphere. The equivalent CH_4 emissions values in the Northern Hemisphere for oil, coal, agriculture/waste/landfills, and natural sources are 91%, 88%, 82%, and 54%, respectively. The observed difference between the most Southern (90°S-72°S) and Northern (72°N-90°N) latitudinal

374 band is 134 ppb (7.6% of the global average CH_4 mixing ratio) compared to 177 ppb (10.1%) in
375 the simulation (medium FER scenario) averaged over 1990-2010, which is qualitatively consistent
376 with previous studies[35,64]. This small North-South (N-S) gradient mismatch between observations
377 and simulation suggests that the simulated CH_4 estimates for each source category could be
378 plausible.
379

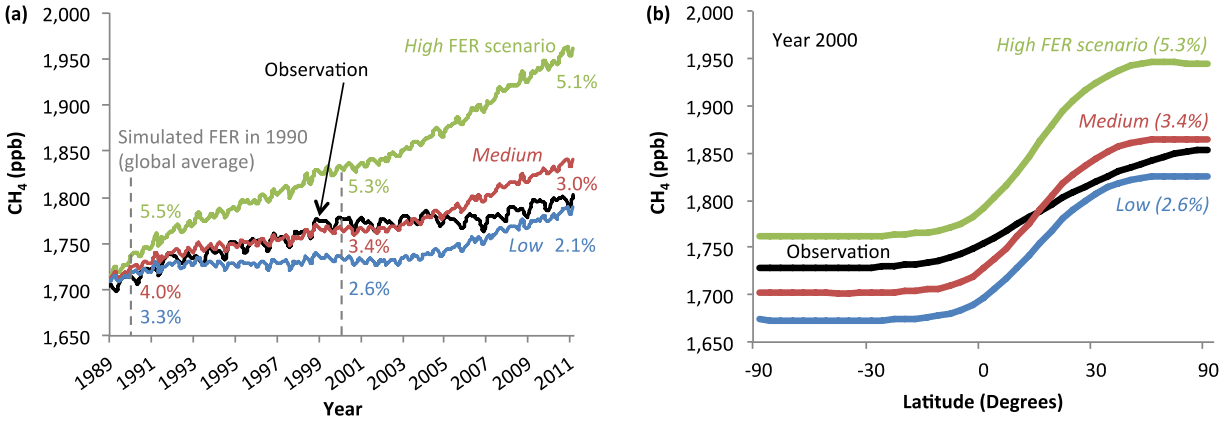

380

381 **Figure 2:** TM5 global average forward modeling results for three regionally and temporally
382 distinct FER scenarios (see SI Table S4 and Figure S9) as well as NOAA's measurements[19]. (**a**)
383 Global average dry air mole fractions; see[65,66] for estimating global averages from spatial
384 distributions. (**b**) CH_4 dry air mole fractions across 41 latitudinal bands in year 2000 (see SI Figure
385 S10 for additional years).

386 The inter-hemispheric gradient indicates that total emissions in the medium FER scenario (best
387 global fit in 2000; see Figure 2a) are too high in the North and too low in the South (relative to the
388 simulated *a priori* dataset). Also, the simulated inter-hemispheric gradient is significantly higher
389 than the observation in all FER scenarios. Because (i) reducing FER alone is not sufficient to match
390 the observed inter-hemispheric gradient, and (ii) coal and oil CH_4 totals are considered a low
391 estimate (i.e., Northern emissions could be even higher), misallocation of non-FF CH_4 emissions

392 across hemispheres must at least partially explain the N-S mismatch. This is consistent with
393 previous atmospheric inversions, which tend to reduce high latitudinal sources compensated by
394 increases at lower latitudes[35,64]. Tropical wetlands may be underestimated in particular[35]. Further
395 evidence is provided in the SI (section 3.2), which illustrates that NG (or other FFs) are unlikely
396 causes of the N-S mismatch between simulations and observations. Instead, seasonal observations
397 suggest that wetlands (a reduction in the North and an increase in the South) and/or
398 agriculture/waste/landfills (an increase in the North) were biased in the *a priori* estimates.

399 **Influence of FER on life cycle GHG emissions of power generation compared with coal**

400 The life cycle GHG emissions from power generation are frequently estimated to assess the
401 feasibility of replacing coal with NG to mitigate climate change[10,11,67–69]. Note, however, that other
402 comparisons, e.g., use as a transportation fuel[70], are also policy-relevant. Corresponding to
403 previous work[10,11,67–69], this study estimates the climate implications of NG in terms of CO_2-
404 equivalent (CO_2e) emissions per unit of generated electricity. This metric accounts for the
405 differences in cumulative radiative forcing of CH_4 relative to CO_2 over a given period – commonly
406 100 and 20 years – using global warming potentials (GWP)[71]. Figure 3 compares total life cycle
407 GHG emissions of power generation from coal and NG assuming 39% and 50% efficiency,
408 respectively. Given a GWP of 28 (100-yr period), and assuming 3% FER (i.e., the mean value of
409 the most likely FER range since 2000 from this study), total NG emissions are about 39% lower
410 than coal. After including climate-carbon feedbacks (CC FB), which account for the impact of the
411 GHGs on other gaseous and aerosol forcing species[71], this value decreases to 36% (GWP 34). The
412 FER would need to be 10% (excluding CC FB; 8.5% FER including CC FB) in order to reach the
413 same total emissions as coal (break-even point). However, over a 20-yr period, NG already breaks
414 even with coal at 3.4% FER, thus well within the most likely FER range in this study. Results for

GWP 84 (20-yr, no CC FB) are not shown in Figure 3 because differences are negligibly small (3.5% break-even FER). Note that this coal-NG comparison excludes potential direct climate effects from non-GHG climate forcers, such as sulfate aerosols from coal combustion, which may have a cooling effect[2].

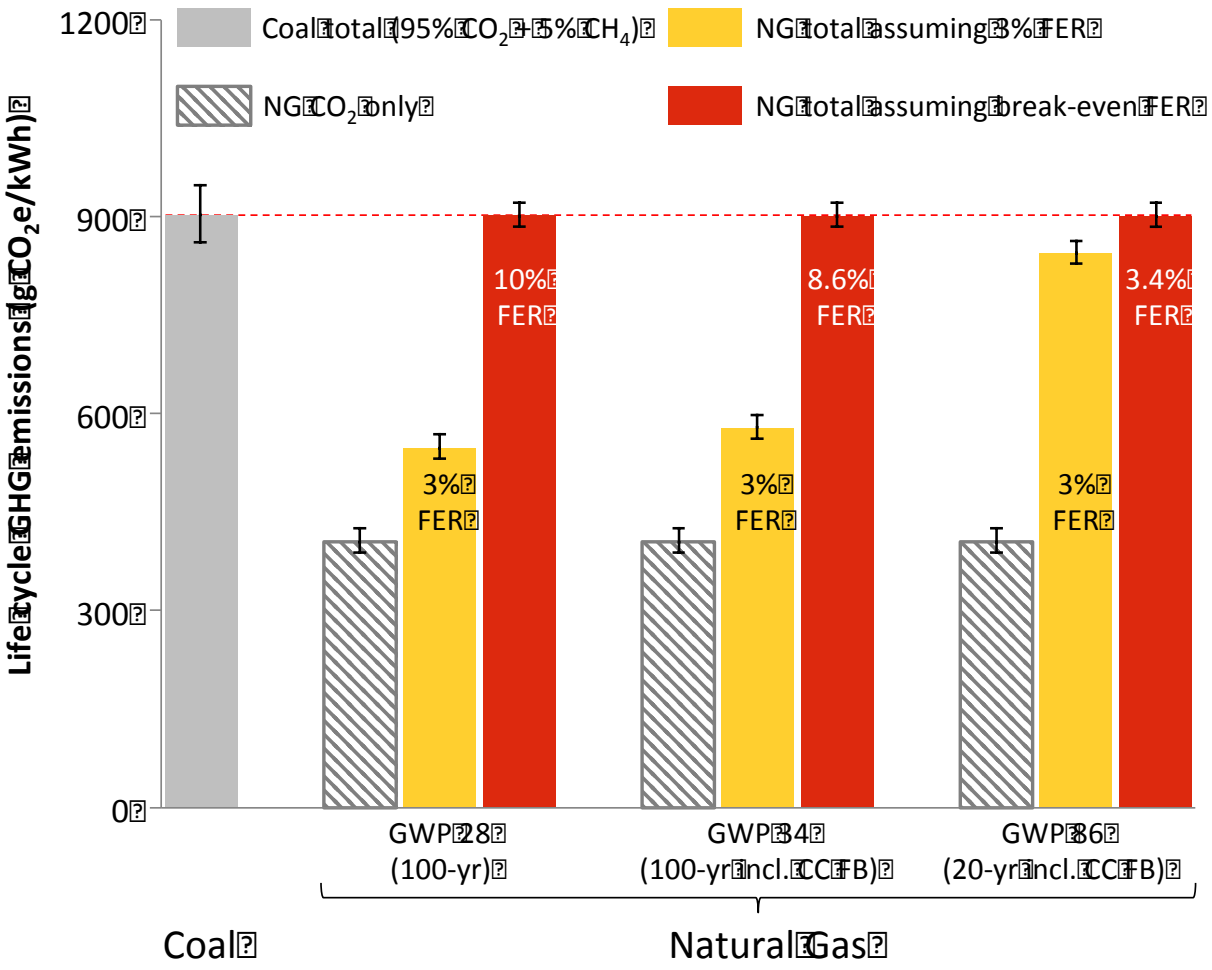

Figure 3: Comparison of life cycle GHG emissions of power generation from coal and NG assuming 39% and 50% conversion efficiency, respectively. Literature estimates for coal[1,2,11] and NG[1,2,10,72] CO_2 were used. Yellow and red columns assume 3% FER (mean value of most likely FER range since 2000 from this study) and break-even FER (required to match coal emissions), respectively, using 48 g CO_2e/kWh per percentage point FER from[68]. NG is shown for three

different global warming potentials (GWP; see text). Coal is shown for GWP 28 only because CH_4 contributes only 5% to total emissions. NG error bars include CO_2 only. Coal error bars pertain to combined uncertainty in CO_2 and CH_4 emissions. CC FB: climate-carbon feedbacks (see text).

Discussion

The objective of this top-down study was to estimate global average FER related to the NG life cycle in order to better understand whether recently reported high FER of 6-9%[1,4] are representative of the larger NG industry. Using a global box-model and well-known quantities of global average atmospheric CH_4, $\delta^{13}C$-CH_4, and C_2H_6 mixing ratios, the most likely FER was found to be 2-4% since 2000, and currently (2006-2011) having an upper bound FER of 5%. Both results are potentially overestimated because these estimates exclude highly uncertain emissions from natural hydrocarbon seepage. Taking into account increasing NG (and other FF) production, the FER (in % of dry production) has been declining steadily over time.

The box-model results (most likely FER of 2-4% since 2000) are consistent with those from 3D modeling. The low magnitude of the difference in the inter-hemispheric gradient between simulations and measurements (less than 5% of the global budget) indicates a minor bias in the simulated emissions sources. The inter-hemispheric gradient and seasonal comparisons show that an improved spatial emissions allocation includes (i) an emissions transfer from Northern to Southern wetland emissions and/or (ii) increased Northern agriculture/waste/landfills emissions in combination with FER lower than 2-4%. Thus neither the inter-hemispheric gradient nor the seasonal comparisons suggest that a global average FER of 2-4% over the period 2000-2011 is too low. This conclusion is subject to potential imprecision of the TM5 emissions transport model, which may lead to uncertainties in the simulated spatial allocation of CH_4 emissions. However, this is unlikely given the independent C_2H_6 based box-model upper bound FER of 5%.

448 The study results lead to both research recommendations and policy implications. A more formal
449 uncertainty analysis of key parameters (atmospheric lifetimes, natural emissions and NG
450 composition) would provide a more detailed characterization of FER uncertainties. This requires
451 composition data by well type (NG, oil) that are not currently available at this level of detail.
452 Policies aimed at providing such data, e.g., publishing international well sample data collected
453 from the oil and gas industry in a central database, would improve the accuracy of FER estimates.
454 The most likely global FER range (2-4%) is slightly higher than many recent bottom-up
455 estimates (1.1-3.2%; full life cycle) in the U.S. and elsewhere[10,51,68,73]; however, potentially
456 unaccounted natural seepage could reduce our estimate. Our most recent (2011) *global* upper
457 bound of 4.4% FER suggests that two recent high estimates of 6-9% in the U.S.[1,4] may be possible
458 at individual sites, but do not appear representative of the national average unless U.S. NG industry
459 practices are significantly worse than in the rest of the world. When used for power generation,
460 combined NG CH_4 and CO_2 emissions break even with coal at 8.6% FER using a 100-year CH_4
461 GWP (including CC FB), but the break-even is only 3.4% over 20 years (Figure 3). Thus, despite
462 our relatively low FER estimates, policies to further reduce fugitive emissions appear justified.
463 Shale gas production was too small globally (increasing from 1.5% of global production in 2007
464 to 5.9% in 2011[61]) to yield a signal *even if* FER from shale gas is higher than from conventional
465 NG. However, few bottom-up studies indicate significantly higher FER from shale compared to
466 conventional gas[68]. Local and regional top-down studies using field measurements can
467 complement global modeling. These may provide more basin specific FER estimates unattainable
468 with the current global observational network. The NG industry average FER estimates from this
469 work can be used as a reference, and basin specific studies may point to areas with local or regional
470 hot spots.

Supporting Information. Literature review of simulated non-FF emissions, observational data description, additional box-model and 3D-model results, and comparison of GHG emissions impacts from NG and coal power generation using global warming potentials. This material is available free of charge via the Internet at http://pubs.acs.org.

Present Addresses

[⊓] NOAA Earth Systems Research Laboratory, 325 Broadway GMD1, Boulder, CO 80305, United States

Author Contributions

S.S. was responsible for study design, development of box-model and emissions inventory, analysis of 3D-model results, and manuscript preparation. W.M.G. and H.S.M. helped with study design, model analysis, and improved the manuscript. L.B. did 3D-modeling, helped with model analysis, and improved the manuscript. All authors have given approval to the final version of the manuscript.

Funding Sources

Climate and Energy Decision Making (CEDM) center through a cooperative agreement between the National Science Foundation (SES-0949710) and Carnegie Mellon University; ERM Foundation-North America Sustainability Fellowship.

Acknowledgment

We thank Ed Dlugokencky and John B. Miller for valuable comments and discussions. The long-term ethane data are from the UC Irvine global monitoring network

(http://cdiac.ornl.gov/trends/otheratg/blake/blake.html). This research was made possible through support from the Climate and Energy Decision Making (CEDM) center. This Center has been created through a cooperative agreement between the National Science Foundation (SES-0949710) and Carnegie Mellon University. The ERM Foundation-North America Sustainability Fellowship has provided additional funding.

Abbreviations

CH_4, methane; C_2H_6, ethane; EF, emissions factor; FER, fugitive emissions rate (% of dry production of NG); FF, fossil fuels (natural gas, oil, coal); GWP, global warming potential; NG, natural gas.

References

1. Howarth, R. W., Santoro, R. & Ingraffea, A. *Clim. Change* **106,** 679–690 (2011).
2. Wigley, T. M. L. *Clim. Change* **108,** 601–608 (2011).
3. Pétron, G. *et al. J. Geophys. Res.* **117,** D04304 (2012).
4. Karion, A. *et al. Geophys. Res. Lett.* **40,** 4393–4397 (2013).
5. Miller, S. M. *et al. Proc. Natl. Acad. Sci.* **110,** 20018–20022 (2013).
6. Brandt, A. R. *et al. Sci.* **343 ,** 733–735 (2014).
7. EPA. *Oil and Natural Gas Sector: Reconsideration of Certain Provisions of New Source Performance Standards, Final Rule, 40 CFR Part 60*. (2013). http://www.gpo.gov/fdsys/pkg/FR-2013-09-23/pdf/2013-22010.pdf
8. Allen, D. T. *et al. Proc. Natl. Acad. Sci. U. S. A.* **110,** 17768–73 (2013).
9. API/ANGA. *Characterizing Pivotal Sources of Methane Emissions from Natural Gas Production: Summary and Analysis of API and ANGA Survey Responses*. (2012).
10. Venkatesh, A., Jaramillo, P., Griffin, W. M. & Matthews, H. S. *Environ. Sci. Technol.* **45,** 8182–8189 (2011).

11. Jiang, M. *et al. Environ. Res. Lett.* **6,** 034014 (2011).

12. Gage, B. D. & Driskill, D. L. *Analyses of natural gases 1917-2007*. (2008).

13. Simpson, I. J. *et al. Nature* **488,** 490–494 (2012).

14. Aydin, M. *et al. Nature* **476,** 198–201 (2011).

15. Levin, I. *et al. Nature* **486,** E3–E4 (2012).

16. Miller, J. B. The carbon isotopic composition of atmospheric methane and its constraint on the global methane budget. In *Stable Isot. Biosph. Interact.* (Flanagan, L. B., Ehleringer, J. R. & Pataki, D. E.) 288–310 (Elsevier, 2005).

17. Kirschke, S. *et al. Nat. Geosci.* **6,** 813–823 (2013).

18. Schwietzke, S., Griffin, W. M. & Matthews, H. S. Global bottom-up fossil fuel fugitive methane and ethane emissions inventory for atmospheric modeling. *ACS Sustainable Chem. Eng.* (2014). Accepted.

19. ESRL. *CarbonTracker-CH4 documentation*. (2013). http://www.esrl.noaa.gov/gmd/ccgg/carbontracker-ch4/documentation_obs.html#ct_doc

20. Prinn, R. G., Huang, J., Weiss, R. F. & Cunnold, D. M. *Geophys. Res. Lett.* **32,** 2–5 (2005).

21. Prather, M. J., Holmes, C. D. & Hsu, J. *Geophys. Res. Lett.* **39,** (2012).

22. Naik, V. *et al. Atmos. Chem. Phys.* **13,** 5277–5298 (2013).

23. Voulgarakis, A. *et al. Atmos. Chem. Phys.* **13,** 2563–2587 (2013).

24. Rudolph, J. *J. Geophys. Res. Atmos.* **100,** 11369–11381 (1995).

25. Hartmann, D. L. *et al.* Observations: Atmosphere and Surface. In *Clim. Chang. 2013 Phys. Sci. Basis. Contrib. Work. Gr. I to Fifth Assess. Rep. Intergov. Panel Clim. Chang.* (Stocker, T. F. et al.), (Cambridge University Press, 2014).

26. Krol, M. *et al. Atmos. Chem. Phys.* **5,** 417–432 (2005).

27. Bruhwiler, L. *et al.* CarbonTracker-CH4: An assimilation system for estimating emissions of atmospheric methane. *Atmos. Chem. Phys.* (2013). Submitted.

28. Fung, I., Prather, M., John, J., Lerner, J. & Matthews, E. *J. Geophys. Res.* **96,** 13033–13065 (1991).

29. Lassey, K. R., Lowe, D. C. & Manning, M. R. *Global Biogeochem. Cycles* **14,** 41–49 (2000).

30. Sriskantharajah, S. *et al. Tellus B; Vol 64* (2012). http://www.tellusb.net/index.php/tellusb/article/view/18818

31. Schoell, M. *Am. Assoc. Pet. Geol. Bull.* **67,** 2225–2238 (1983).

32. Michel, S. E. Institute of Arctic and Alpine Research (INSTAAR), University of Colorado, Boulder. *Personal communication*. (2014).

33. Miller, J. B. *et al. J. Geophys. Res. Atmos.* **107,** ACH 11–1–ACH 11–15 (2002).

34. EIA. *International Energy Statistics*. (2013). http://www.eia.gov/cfapps/ipdbproject/iedindex3.cfm?tid=2&pid=38&aid=12&cid=regions&syid=1980&eyid=2011&unit=BKWH

35. Mikaloff Fletcher, S. E., Tans, P. P., Bruhwiler, L. M., Miller, J. B. & Heimann, M. *Global Biogeochem. Cycles* **18,** GB4004 (2004).

36. Bousquet, P. *et al. Nature* **443,** 439–43 (2006).

37. Chen, Y.-H. & Prinn, R. G. *J. Geophys. Res. Atmos.* **111,** (2006).

38. Wang, J. S. *et al. Global Biogeochem. Cycles* **18,** (2004).

39. IPCC. *Climate Change 2001: The Physical Science Basis. Contribution of Working Group I to the Third Assessment Report of the Intergovernmental Panel on Climate Change. Chapter 6*. (2001).

40. Wuebbles, D. J. & Hayhoe, K. *Earth-Science Rev.* **57,** 177–210 (2002).

41. Ridgwell, A. J., Marshall, S. J. & Gregson, K. *Global Biogeochem. Cycles* **13,** 59 (1999).

42. Bergamaschi, P. *et al. J. Geophys. Res.* **112,** 1–26 (2007).

43. Janssens-Maenhout, G. *et al. EDGAR-HTAP: a harmonized gridded air pollution emission dataset based on national inventories*. (2012).

44. Matthews, E., Fung, I. & Lerner, J. *Global Biogeochem. Cycles* **5,** 3 (1991).

45. Giglio, L., Van Der Werf, G. R., Randerson, J. T., Collatz, G. J. & Kasibhatla, P. *Atmos. Chem. Phys.* **6,** 957–974 (2006).

46. Van Der Werf, G. R. *et al. Atmos. Chem. Phys. Discuss.* **6,** 3175–3226 (2006).

47. GFED. *Global Fire Emissions Database*. (2013). http://www.globalfiredata.org/

48. Elvidge, C. D. *et al. Energies* **2,** 595–622 (2009).

49. Elvidge, C. D., Baugh, K. E., Ziskin, D., Anderson, S. & Ghosh, T. *Estimation of Gas Flaring Volumes Using NASA MODIS Fire Detection Products*. (2011).

50. IPCC. *2006 IPCC Guidelines for National Greenhouse Gas Inventories, Prepared by the National Greenhouse Gas Inventories Programme*. *Agric. For. Other L. Use* **4,** (IGES, 2006).

51. EPA. *Inventory of U.S. Greenhouse Gas Emissions and Sinks: 1990 – 2011*. (2013). http://www.epa.gov/climatechange/ghgemissions/usinventoryreport.html

52. Wilson, D., Fanjoy, J. & Billings, R. *Gulfwide Emission Inventory Study for the Regional Haze and Ozone Modeling Effort*. (2004).

53. Wilson, D. *et al. Year 2008 Gulfwide Emission Inventory Study*. (2010).

54. EPA. *Reducing Methane Emissions From Coal Mines in China: The Potential for Coalbed Methane Development*. (1996).

55. CIRI. *China Coal Industry Yearbook 2009*. (2011).

56. EPA. State Inventory and Projection Tool. (2012). http://www.epa.gov/statelocalclimate/resources/tool.html

57. Fung, I., Matthews, E. & Lerner, J. *Abstr. Pap. Am. Chem. Soc.* **193,** 6–GEOC (1987).

58. Kaplan, J. O. *Geophys. Res. Lett.* **29,** 3–6 (2002).

59. Etiope, G. & Ciccioli, P. *Science (80-.).* **323,** 478 (2009).

60. Nisbet, E. G., Dlugokencky, E. J. & Bousquet, P. *Sci.* **343 ,** 493–495 (2014).

61. EIA. *U.S. Energy Information Administration*. (2014). www.eia.gov

62. Montzka, S. A. *et al. Science* **331,** 67–69 (2011).

63. Dlugokencky, E. J., Nisbet, E. G., Fisher, R. & Lowry, D. *Philos. Trans. R. Soc. - Ser. A Math. Phys. Eng. Sci.* **369,** 2058–2072 (2011).

64. Houweling, S., Kaminski, T., Dentener, F., Lelieveld, J. & Heimann, M. *J. Geophys. Res.* **104,** 26137–26160 (1999).

599 65. Dlugokencky, E. J., Steele, L. P., Lang, P. M. & Masarie, K. A. *J. Geophys. Res.* **100,**
600 23103 (1995).

601 66. Masarie, K. A. & Tans, P. P. *J. Geophys. Res.* **100,** 11593 (1995).

602 67. NETL. *Life Cycle Greenhouse Gas Inventory of Natural Gas Extraction, Delivery and*
603 *Electricity Production*. (2011).

604 68. Weber, C. L. & Clavin, C. *Environ. Sci. Technol. Technol.* **46,** 5688–5695 (2012).

605 69. Burnham, A. *et al. Environ. Sci. Technol.* **46,** 619–627 (2012).

606 70. Alvarez, R. A., Pacala, S. W., Winebrake, J. J., Chameides, W. L. & Hamburg, S. P. *Proc.*
607 *Natl. Acad. Sci. U. S. A.* **109,** 6435–40 (2012).

608 71. Myhre, G. *et al.* Anthropogenic and Natural Radiative Forcing. In *Clim. Chang. 2013*
609 *Phys. Sci. Basis. Contrib. Work. Gr. I to Fifth Assess. Rep. Intergov. Panel Clim. Chang.*
610 (Stocker, T. F. et al.) (Cambridge University Press, 2014).

611 72. Jaramillo, P., Griffin, W. M. & Matthews, H. S. *Environ. Sci. Technol.* **41,** 6290–6296
612 (2007).

613 73. Dienst, C. *et al. Treibhausgasemissionen des russischen Exportpipeline System –*
614 *Ergebnisse und Hochrechnungen empirischer Untersuchungen in Russland*. (2004).

615

616 **TOC/Abstract art**

617